

Methods for Determination of Response Times of Magnetic Head Materials

T. J. Silva and T. M. Crawford

National Institute of Standards and Technology, Boulder, Colorado, USA

Abstract—Measurements of magnetization response times in thin-film Permalloy are made by both electrical and optical methods. The electrical method measures the inductive voltage generated in a waveguide by the changing magnetization. The optical technique uses standard pump-probe sampling methods combined with the second-harmonic magneto-optic Kerr effect to directly measure magnetization angle as a function of time. Results of these measurements for a 75 nm thick Permalloy film are in good qualitative agreement.

Index Terms—Coplanar waveguide, inductive voltage, Landau-Lifshitz damping, magnetic switching speed, magneto-optic sampling, second-harmonic magneto-optic Kerr effect.

I. INTRODUCTION

Continued increases in disk-drive data rates are raising the question: What fundamental physical limits restrict the bandwidth of the magnetic components in a thin-film head? Studies of ferromagnetic resonance (FMR) suggest that the fastest magnetic switching speeds for thin films occur at rates determined by the gyromagnetic ratio γ via the standard FMR resonance frequency relation:

$$\omega_p = \gamma\mu_0 \sqrt{\frac{\partial^2 U}{\partial \phi^2}}, \quad (1)$$

where U is the magnetic free energy, ϕ is the in-plane magnetization angle, μ_0 is the permeability of free space, and ω_p is the precession frequency in rad/s [1]. The gyromagnetic ratio is typically $\gamma = 1.76 \times 10^{11}$ rad/(T·s). For a uniformly magnetized film with saturation magnetization M_s and uniaxial magnetocrystalline anisotropy H_k , (1) reduces to

$$\omega_p = \gamma\mu_0 \sqrt{M_s H_k}. \quad (2)$$

For conventional Permalloy, we calculate a resonance frequency of $f_p = \omega_p/2\pi = 630$ MHz. Using the usual criteria for a 10%-90% switching speed, we obtain a minimum theoretical switching time of $t_s = 0.35/f_p = 600$ ps. This raises concern since extrapolation of disk drive data rates over the last 10 years predicts that the time constant of the heads will need to approach 200 ps by 2005 [2].

While traditional FMR methods provide an excellent means to determine a material's fundamental gyromagnetic properties through Eq. (1), excitation amplitudes are insufficient to test the validity of an extrapolated switching speed. To this end, we have constructed two instruments for the temporal measurement of ultrafast magnetodynamics with resolutions of 20-30 ps. The first instrument is purely

electrical, using the inductive voltage produced during magnetic switching to provide a measurable signal [3]. The second is optical, relying upon a nonlinear form of the magneto-optic Kerr effect (MOKE) for magnetic contrast [4].

II. METHODS

A. Inductive Technique

A schematic of the inductive instrument is shown in Fig. 1. The method is conceptually similar to instruments used in the 1950s to investigate switching speeds in thin film Permalloy [5]. A complete description of the system may be found in [3]. In-plane magnetic field pulses are delivered to the sample with a coplanar waveguide structure lithographically fabricated on a polymeric dielectric substrate. A microwave pulse generator provides voltage steps to the 50 Ω matched waveguide structure. We employ a commercial pulse generator with a nominal 50 ps risetime, a 10 V amplitude, and a 10 ns duration. The sample is placed on top of the center conductor of the waveguide, where it is subjected to an in-plane magnetic field pulse as the voltage step travels along the waveguide. The field pulse is transverse to the propagation direction. For zero separation between the waveguide and sample, we may use the well-known result for the fields above a uniform current sheet: $H_p = I/2w$, where w is the width of the waveguide. The coplanar waveguide has a center conductor width of 0.5 mm. Thus, we would expect fields as large as $H_p = 200$ A/m (2.5 Oe) if we could place the sample in direct contact with the waveguide. The crystalline anisotropy axis of the sample is aligned in the direction of pulse propagation. Helmholtz coils are used to provide a dc bias field H_b along the anisotropy direction to both stabilize the sample magnetization and alter the precessional dynamics.

The sample is 75 nm thick Permalloy, which is sputtered on 100 μm thick Si. The film was deposited in a magnetic field to induce an in-plane easy axis with an anisotropy of $H_k \approx 320$ A/m (4 Oe). The saturation magnetization M_s was measured using a SQUID magnetometer to determine the anisotropy of the sample perpendicular to the film plane, with the result $M_s = 814$ kA/m (814 emu/cm³). The Permalloy was patterned into a stripe 250 μm wide and 4 mm long (a 16:1 aspect ratio). The narrow stripe width facilitated placement of the sample directly over the center of the waveguide where the magnetic fields are maximum. The sample was taped onto the waveguide, with the Si substrate lying between the Permalloy and the waveguide, to facilitate optical measurements of the dynamics.

As the magnetization of the sample rotates under the influence of the field pulse, the resultant flux produced transverse to the waveguide induces a "back emf" voltage

Manuscript received June 30, 1998.

T. J. Silva, 303-497-7826, fax 303-497-5316, silva@boulder.nist.gov; T. M. Crawford, 303-497-3701, fax 303-497-5316, crawford@boulder.nist.gov. Contribution of National Institute of Standards and Technology, not subject to copyright.

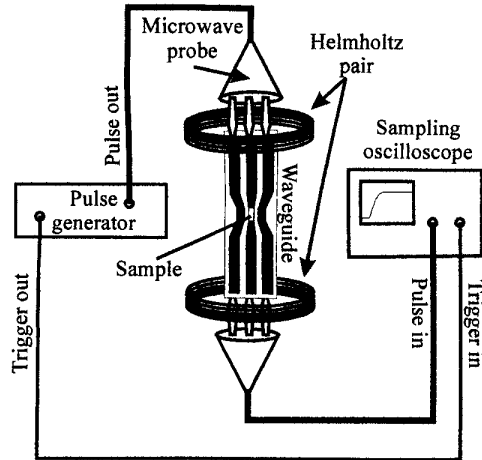


Fig. 1. Schematic of inductive measurement system.

pulse $V_p = d\Phi/dt$. The measured voltage is related to the average transverse magnetization M_y by

$$\overline{M}_y = \frac{4}{\mu_0 \delta l \epsilon} \int V_p dt, \quad (3)$$

for a sample of thickness δ and length l [3]. The inductive coupling efficiency ϵ describes the actual linkage of flux between the sample and the waveguide. For a sample with uniform magnetization which is in direct contact with the waveguide center conductor, we expect $\epsilon = 1$. We estimate ϵ by use of reciprocity as

$$\epsilon = \frac{2 \int_{\text{sample}} h_y(\vec{r}) dr}{\delta l}, \quad (4)$$

where h_y is the transverse component of magnetic field produced by the waveguide for a unit excitation current [3]. We assume that the normal component of magnetization is approximately 0 due to the large demagnetization factor perpendicular to the film plane.

The inductive voltage pulse propagates through the waveguide along with the driving voltage pulse into a sampling oscilloscope with a 20 GHz bandwidth. Saturation of the sample with an external field parallel to H_p produced by additional Helmholtz coils (not shown in Fig. 1) allows for a background measurement of the nonmagnetic response in the waveguide. The background signal is then subtracted from subsequent traces. An oscilloscope with high dynamic range must be used because the inductive signal is typically 60 dB smaller than the background of the voltage step.

B. Optical Technique

A schematic of the optical measurement system is shown in Fig. 2. The same excitation system is used as for the inductive method. The magnetization state of the Permalloy is sampled magneto-optically in a fashion similar to that employed by Freeman and coworkers [6]. The delay between the microwave pulse and the incident laser pulse is adjusted using an electronic delay generator with an rms jitter of 40 ps.

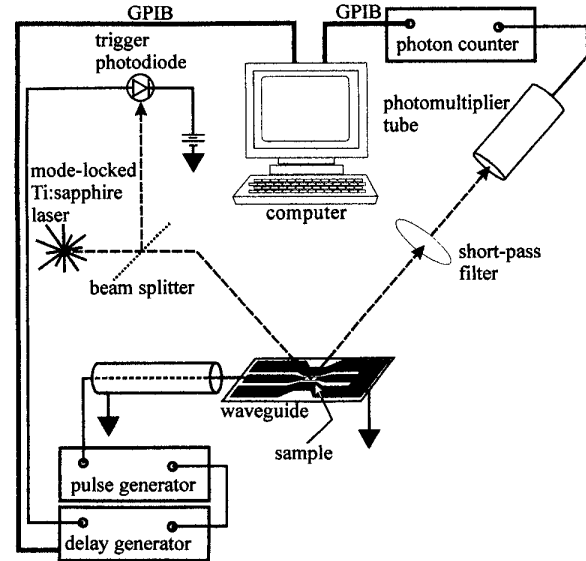


Fig. 2. Schematic of nonlinear optical measurement system. Helmholtz coils used to produce the longitudinal bias field H_b are not shown.

The delay generator was calibrated with the same sampling oscilloscope used for the inductive measurements to guarantee consistency of the time base used for the two measurements, with a measured uncertainty of ≈ 50 ps. Over a 6 ns delay time, this produces a time base error of $\approx 1\%$.

Our laser source is a commercial mode-locked Ti:sapphire laser which produces 60 fs pulses at an 800 nm wavelength. The laser pulses are focused onto the sample surface to approximately a $10 \mu\text{m}$ spot size, producing peak power densities in excess of $100 \text{ GW}/\text{cm}^2$. At such high electric fields, the Permalloy surface acts as a second-harmonic generator, producing a collinear reflected pulse at half the wavelength of the incident pulse. The second-harmonic generation (SHG) efficiency of Permalloy has a strong magnetic contrast of approximately 50% [7]. This second-harmonic magneto-optic Kerr effect (SH-MOKE) directly measures the magnetization transverse to the plane of incidence in the sample plane. The sample is oriented so that the waveguide is parallel to the incidence plane; that is, we measure the component of magnetization orthogonal to the Permalloy stripe. The poor SHG efficiency of Permalloy produces photon yields of 100 counts per second, requiring long averaging times. Given the limited signal-to-noise ratio of the optical system, it is advantageous to produce large field pulses at the sample. To this end, the waveguide is terminated with a short, producing field pulses of $2H_p$ due to the reflected pulse.

The $10 \mu\text{m}$ diameter spot size represents a compromise between the desire to maximize SHG and the requirement for signal stability. At smaller spot sizes, SHG yield was not stable over the many hours required to complete a measurement. The instability is in part due to increased surface oxidation of the Permalloy at elevated temperatures [8]. A stable signal indicates that sample temperatures are significantly less than 100°C [8]. In addition, M_s is only weakly affected by such a slight temperature increase.

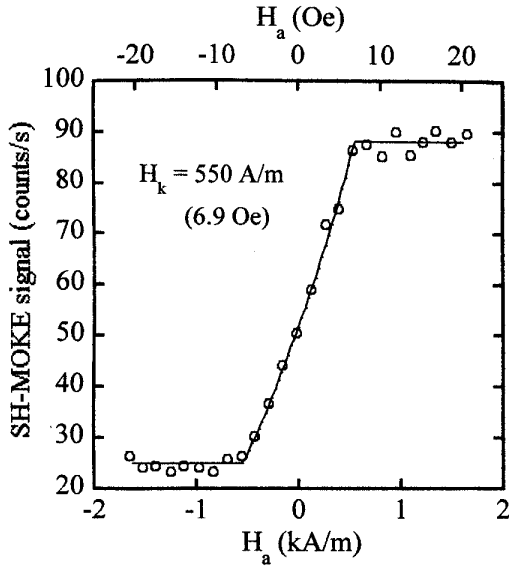


Fig. 3. Hard-axis hysteresis loop measured by SH-MOKE. Such loops are used to calibrate time-resolved measurements. Open circles are data; solid line is a fit to (6). The nonlinearity in the data for $|H_a| < 560$ A/m (7 Oe) is due to a quadratic dependence upon M_y for transverse SH-MOKE.

To calibrate the SHG signal as a function of sample magnetization, we perform static SH-MOKE hysteresis measurements using Helmholtz coils to produce a magnetic field H_a parallel to the pulsed fields from the waveguide. As such, the measured loop constitutes a hard axis measurement. We assume that the magnetization is a linear function of applied field for $|H_a| < H_k$ and is equal to M_s otherwise. We then fit the data to ascertain the anisotropy and SHG efficiency of the sample.

Such calibration measurements are somewhat complicated due to the nature of the large contrast for SH-MOKE. The SHG output of the sample for the transverse geometry is given by

$$I(2\omega) = C \left| \chi_{nm}^{(2)} + \chi_m^{(2)} \right|^2 I^2(\omega), \quad (5)$$

where $I(\omega)$ is the peak intensity of the incident laser; $\chi_{nm}^{(2)}$ is an effective second-order susceptibility tensor component which describes nonmagnetic contributions to the SHG; $\chi_m^{(2)}$ is an effective second-order susceptibility tensor component which is linear in magnetization; C is a proportionality constant that accounts for laser repetition rate, pulse duration and spot size; and $I(2\omega)$ is the intensity of the total second harmonic produced by the sample [9]. Both second order susceptibility tensor components are complex quantities that are mixtures of elemental tensor components, each of which is weighted by appropriate factors to account for the angle of incidence and refractive index of the sample. If we expand (5), we find

$$I(2\omega) \propto \left| \chi_{nm}^{(2)} \right|^2 + \left| \chi_m^{(2)} \right|_{\max}^2 m^2 + 2 \cos(\varphi) \left| \chi_{nm}^{(2)} \right| \left| \chi_m^{(2)} \right|_{\max} m, \quad (6)$$

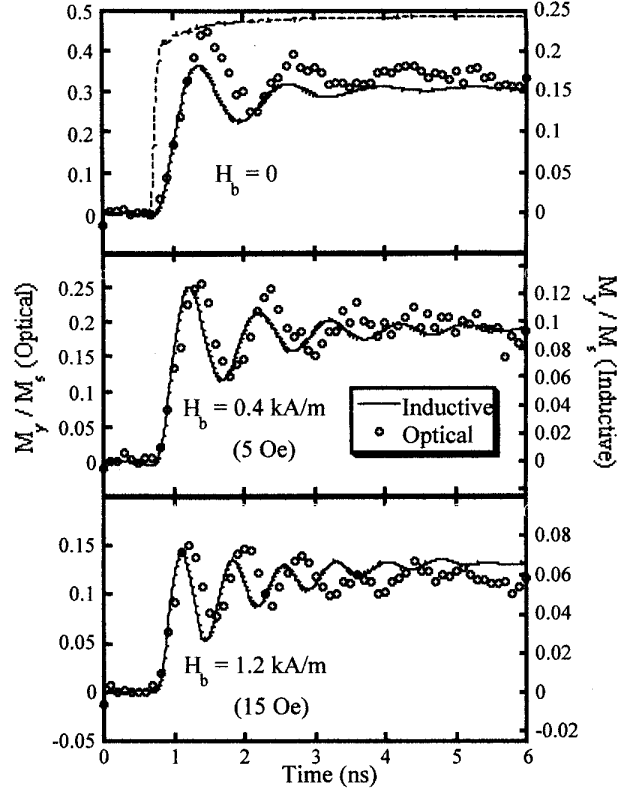


Fig. 4. Traces of magnetization as a function of time, as determined by both optical and inductive techniques. Solid line are the inductive data, open circles are the optical data. A trace of the voltage pulse transmitted through the waveguide is shown in the upper plot as a dashed curve. We assume the field pulse is linearly proportional to the voltage pulse.

where $m = M_y/M_s$ and $\varphi = \arg(\chi_{nm}^{(2)}) - \arg(\chi_m^{(2)})$. Thus, we see that the SH-MOKE contrast has a quadratic dependence upon sample magnetization which cannot be ignored in the case of large contrast, that is, when $\chi_m^{(2)}/\chi_{nm}^{(2)} \approx 1$. Since an absolute determination of the tensor components is difficult and subject to assumptions as to which elemental tensor components compose the effective admixtures, we fit only the ratio $\chi_m^{(2)}/\chi_{nm}^{(2)}$. In fact, an absolute calibration is unnecessary since we want only to determine the proportionality of $I(2\omega)$ to M_y . An example of a SH-MOKE loop and fit is shown in Fig. 3. The loop shape is indeed nonlinear in the unsaturated regime $|H_a| < H_k$. The nonlinearity is well described by (6) in a manner which is self-consistent with the large size of SH-MOKE contrast. The resulting fitted parameter values are $\chi_m^{(2)}/\chi_{nm}^{(2)} = 0.31$, $H_k = 550$ A/m (6.9 Oe), and $\varphi = 0$.

The ability to calibrate the sensitivity of time-resolved SH-MOKE is a great advantage of the optical technique over the inductive method.

III. RESULTS

Optical and inductive data are shown in Fig. 4 for several bias fields. The inductive data have been integrated using (3)

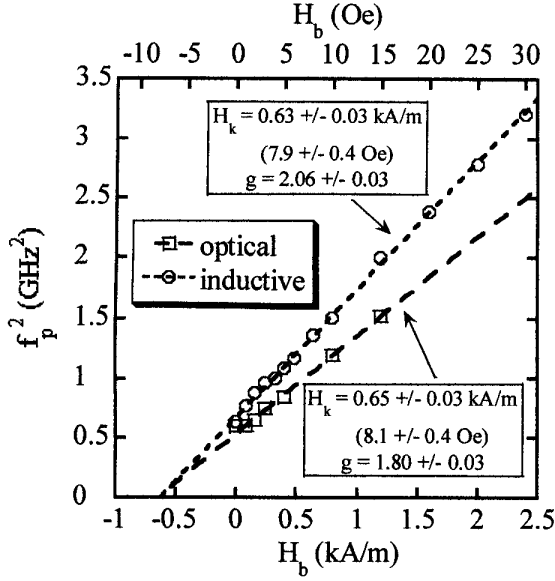


Fig. 5. Squared precessional frequency as a function of longitudinal bias field. Filled circles were measured using the optical method, open circles are obtained by the inductive method. The linear fit is used to extract H_k and gyromagnetic splitting ratio g . The slope is proportional to g and the intercept with the $f_p^2 = 0$ axis is $-H_k$. Error bars are approximately the size of the data symbols.

to facilitate comparison with the optical results. Measured values of M_s , δ and l were used for the integration. Since the exact separation between the sample and waveguide was unknown, (3) could not be used to estimate ϵ . Instead, we estimated ϵ using the optically-measured final value for M_y/M_s , with the result $\epsilon = 0.24$. Note that the inductive data have been magnified by a factor of two relative to the optical data to account for the larger field pulse used for the optical measurement.

Switching speeds for $H_b = 0$ measured by both techniques were comparable. The optical method yielded a 10%-90% switching time of $t_s = 550$ ps. The inductive method produced a faster value of $t_s = 440$ ps. We observe underdamped behavior of the precessional oscillations by both optical and inductive methods. The frequency of precession f_p is distinctly different for the optical and inductive traces. The dynamical anisotropy H_k was determined by measuring f_p for multiple time traces obtained for different H_b and fitting the results using (1). The results are shown in Fig. 5, where we have plotted f_p^2 vs. H_b . In the limit of $H_b + H_k \gg H_p$, (1) reduces to

$$f_p^2 \approx \left(\frac{\mu_0 \gamma}{2\pi}\right)^2 M_s (H_b + H_k) \left[1 + \left(\frac{H_p}{H_b + H_k}\right)^2\right]. \quad (7)$$

Linear fits to the data are also shown in Fig. 5. The value of the reduced χ^2 for the optical fit is 0.2 and for the inductive, 0.3. The difference in f_p between the optical and inductive techniques cannot be explained by the different values of H_p between the two methods, since f_p is still different for large H_b where the effect of H_p is insignificant.

Both the anisotropy and gyromagnetic ratio may be extracted from the linear fit in Fig. 5 by reference to (7). The different slopes between the two sets of data indicate that

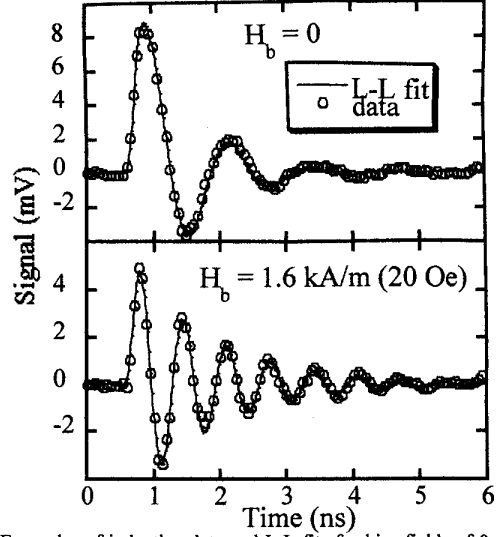


Fig. 6. Examples of inductive data and L-L fits for bias fields of 0 and 1.6 kA/m (20 Oe). Parameters used for the fits are discussed in the text.

dissimilar values for γ must be applicable. We fitted the dimensionless gyromagnetic splitting factor g , defined as

$$g = \frac{\gamma \hbar}{\mu_B}. \quad (8)$$

The fitted values for g are 2.06 ± 0.03 for the inductive data and 1.80 ± 0.03 for the optical data, a difference of 11%.

The intercept of the linear fit to the $f_p^2 = 0$ axis is a dynamical measure of anisotropy, yielding $H_k = 630 \pm 30$ A/m (7.9 ± 0.4 Oe) and $H_k = 650 \pm 30$ A/m (8.1 ± 0.4 Oe) by inductive and optical methods, respectively. The large value of H_k relative to the bulk, static value of 320 A/m (4 Oe) is presumably due to shape anisotropy effects. The dynamical shape anisotropy component H_k^s may be estimated using

$$H_k^s = \frac{n\pi}{2} \left(\frac{M_s \delta}{w}\right), \quad (9)$$

where n is the effective mode number of the dynamical excitation. For the lowest order excitation, $n = 0.735$ [10]. For our sample, we estimate $H_k^s = 280$ A/m (3.5 Oe), in close agreement with our measured values.

We may also analyze our data by fitting the measured waveforms to the integrated Landau-Lifshitz (L-L) equation. We use the SI form of L-L:

$$\frac{d\vec{M}}{dt} = -|\gamma|\vec{T} - \frac{\lambda}{\mu_0 M_s^2} (\vec{M} \times \vec{T}), \quad (10)$$

where \vec{T} is the torque exerted upon the magnetization, defined as $\vec{T} = -\vec{r} \times \vec{\nabla} U$. Such a fit provides additional information concerning the phenomenological damping parameter λ , which has units of s^{-1} . The commonly used, dimensionless Landau-Lifshitz-Gilbert damping constant α is related to λ by

$$\alpha = \frac{\lambda}{\gamma \mu_0 M_s}. \quad (11)$$

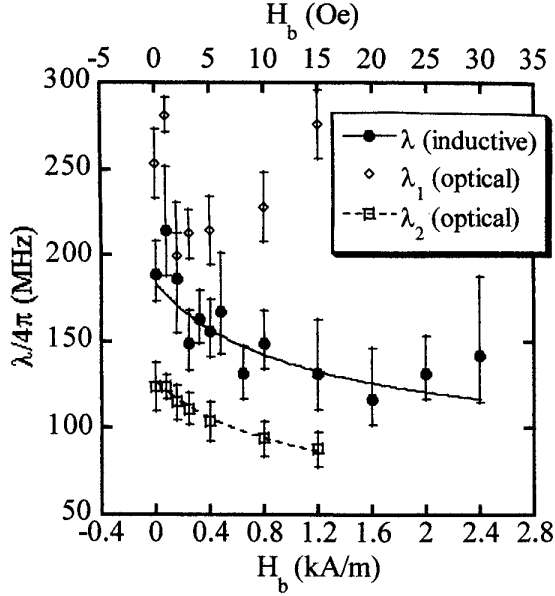


Fig. 7. Landau-Lifshitz damping as a function of H_b . Filled circles were obtained from inductive data. Open diamonds and squares were obtained from optical data. The optical data were fitted with a two-stage model for damping. Lines drawn through the data for λ (inductive) and λ_2 (optical) are fits to an inhomogeneity model, described in Section IV.

Note that in this SI definition of L-L, λ is 4π times greater than in previous definitions [1], [3]. We shall quote damping values as $\lambda/4\pi$ to facilitate comparison with past literature. In the limit of small excitations, where the magnetization excursion angle ϕ is small ($\phi \ll 1$), λ is easily related to the exponential damping time of the magnetic precession τ as $\tau = 2/\lambda$.

Details of the fitting procedure are described elsewhere [3], [4]. For the inductive data, such a fit is made with γ , λ , and ϵ as fitting parameters. Unintegrated inductive voltage waveforms were used for the fitting. Integrated waveforms made the fits more susceptible to low frequency ($1/f$) drift in the inductive signals. The amplitude of the fit was adjusted with ϵ . The precessional frequencies were fitted by adjusting γ . We fixed H_k to the value obtained from the linear fit to the inductive data shown in Fig. 5. This was necessary because γ and H_k are not orthogonal within the context of the nonlinear least-squares fit for inductive data. The pulsed field amplitude was extracted from our optical measurements using single-domain Stoner-Wohlfarth theory, with the result $H_p = 110$ A/m (1.4 Oe) [4].

For the optical data, the fitting parameters were γ , H_k , and λ . In this case, the amplitude of the fit was primarily adjusted through H_k , since the ratio $H_p/(H_k + H_b)$ approximately sets the magnitude of magnetic rotation for the fit.

Examples of several fits for inductive data are shown in Fig. 6. The fits are good, with an rms error of 0.2 mV. The fits for the optical data are of similar quality [4].

When fitting the optical data to L-L, we found that the fit could be improved by 20-30% when a two-stage damping model was used. The two-stage damping model uses a different value for λ during the first half-cycle of magnetic

excitation than is used for the rest of the fitting. The first and second stage of damping are described by λ_1 and λ_2 . We have previously observed such phenomena with narrower 50 μm Permalloy stripes measured inductively [3]. In the present case, a two-stage damping model did not improve the fitting of the inductive data.

The results of the L-L fitting for λ may be found in Fig. 7. The first stage of optical damping is roughly 2.5 times greater than λ_2 . The inductive damping lies between the first- and second-stage optical damping. Indeed, if a single damping parameter is used to fit the optical data, values almost identical to the inductive results are obtained. The inductive damping drops monotonically as H_b is increased. The second stage of optical damping tracks λ (inductive) with changing bias field, though with an offset of ~ 60 MHz. The smallest value of λ is obtained optically at $H_b = 1.2$ kA/m (15 Oe), where $\lambda_2/4\pi = 88$ MHz, or $\alpha = 0.006$. Such low damping has been observed for Permalloy in the past using FMR and more recently using time-resolved polar Kerr microscopy [11], [12]. The first stage of optical damping shows no trend to within error bars, with an average value of $\lambda_1/4\pi = 240 \pm 30$ MHz.

The fitted inductive coupling efficiency ϵ showed no trend as a function of H_b . The average value is $\epsilon = 0.24 \pm 0.04$. The fitted H_k for the optical data also showed no trend, with an average value of 620 ± 60 A/m (7.8 Oe ± 0.7 Oe).

IV. DISCUSSION

A. Inductive Coupling

The low value for the inductive coupling efficiency of $\epsilon = 0.24$ is the result of both a narrow magnetic sample and large spacing between the sample and waveguide. To see how this is the case, let us assume that the transverse component of the magnetic field produced by the waveguide is approximately uniform throughout the volume of the sample. Then (4) may be written as

$$\epsilon = 2w_s h_y(z), \quad (12)$$

where w_s is the width of the sample and z is the distance between the sample and the waveguide. While z is not well known, we may use the fitted pulsed field amplitude of $H_p = 1.4$ Oe:

$$\begin{aligned} \epsilon &= \frac{2w_s h_y(z)}{h_y(0)} h_y(0) \\ &= \frac{w_s}{w} \left(\frac{H_y(z)}{H_y(0)} \right) \end{aligned} \quad (13)$$

with the result $\epsilon = 0.28$. Thus we see that the pulse amplitude resulting from a fit to the optical data and the inductive coupling efficiency obtained from a fit to the inductive data are self-consistent.

Using the Karlqvist equations for the magnetic fields produced by a uniform current sheet of width w , we estimate the sample to waveguide spacing to be $z = 220$ μm [12]. We

presume that the additional spacing beyond the thickness of the sample substrate (100 μm) is due to an incomplete attachment of the sample to the waveguide.

At this separation, the transverse field varies by 9% across the width of the sample. Thus, a calculation of ϵ using (13) will be in error by only 10%.

B. Precession Frequency

The differences between inductive and optical precession frequencies are characterized primarily as a difference in the fitted gyromagnetic ratios. Since the same sampling oscilloscope is used to calibrate the time base for the optical technique as is used to conduct the inductive measurements, a time base error of the magnitude required to explain differences in f_p is extremely unlikely. Similarly, the same Hall probe is used to measure H_b for both series of measurements, using sample to probe spacings much smaller than the radius of the Helmholtz coils, making errors in H_b insignificant.

It has been argued that SH-MOKE should exhibit extreme surface sensitivity by virtue of its symmetry properties [14]. If this is indeed the case for the measurements presented here, then the volume sampled by the optical technique is six orders of magnitude smaller than that measured inductively. Therefore, it is not surprising that the two methods may reveal subtle differences in a sample due to some inhomogeneity in sample properties. More data are needed in order to determine whether such presumed inhomogeneities are of a surface or bulk nature.

C. Damping

Past measurements have found that damping typically lessens with increased f_p [3], [15]. This has been attributed to inhomogeneity in H_k [15]. An inhomogeneous contribution, λ_{inh} to the damping should have the form

$$\begin{aligned}\lambda_{\text{inh}} &= 4\pi \frac{\partial\omega_p}{\partial H_k} \frac{\Delta H_k}{H_k} \\ &= 2\pi\gamma\mu_0 \sqrt{\frac{M_s}{H_k}} \frac{\Delta H_k}{\sqrt{1+(H_b/H_k)}}\end{aligned}\quad (14)$$

where ΔH_k is the half width of a Lorentzian distribution for anisotropy [15]. The total damping λ is then $\lambda = \lambda_0 + \lambda_{\text{inh}}$, where λ_0 is an intrinsic damping. We fit (14) to the inductive damping and second stage of optical damping, with the results shown in Fig. 7. The fitted parameters are $\Delta H_k = 34 \pm 7$ A/m (0.42 ± 0.09 Oe), $\lambda_0/4\pi = 60 \pm 20$ MHz and $\Delta H_k = 28 \pm 2$ A/m (0.35 ± 0.03 Oe), $\lambda_0/4\pi = 29 \pm 9$ MHz for the inductive and optical data, respectively. In a simple picture of inhomogeneous broadening where we consider the Permalloy to be an ensemble of independent harmonic oscillators with a dispersion in the resonance frequencies, we would expect λ_{inh} to be smaller for a local measurement than for a macroscopic average. However, we observe the opposite, with very similar values for $\lambda_{\text{inh}} \propto \Delta H_k$ and dissimilar results for λ_0 , which we do not usually presume to

be a spatially varying quantity. Such a result seems to invalidate a simple inhomogeneous picture, which is indeed flawed: The large exchange coupling within the sample strongly violates the assumption of independent oscillators.

V. CONCLUSION

Dynamical data obtained with the inductive and optical techniques generally agree in a broad qualitative sense. Both methods produce results which indicate precession-limited switching followed by underdamped oscillatory "ringing" for the range of parameters we have employed. Subtle quantitative differences between the optical and inductive techniques point toward local inhomogeneities in the magnetic properties of the sample. However, conclusive evidence in this regard remains wanting.

ACKNOWLEDGMENT

The authors are grateful for the helpful guidance of Charles Rogers and Ron Goldfarb. Tony Kos aided with the electrical engineering of both optical and electrical systems.

REFERENCES

- [1] D. O. Smith, "Magnetization reversal and thin films," *J. Appl. Phys.*, vol. 29, pp. 264-273, March 1958.
- [2] K. Klassen, "High Speed Magnetic Recording," 7th Joint MMM-Intermag Conference, San Francisco, 1998, paper GA-01.
- [3] T. J. Silva, C. S. Lee, T. M. Crawford, C. T. Rogers, "Inductive measurement of ultrafast magnetization dynamics in thin-film Permalloy," submitted to *J. Appl. Phys.*
- [4] T. M. Crawford, T. J. Silva, C. T. Rogers, "Magnetization dynamics studied by the second-harmonic magneto-optic Kerr effect," unpublished.
- [5] W. Dietrich and W. E. Proebster, "Millimicrosecond magnetization reversal in thin magnetic films," *J. Appl. Phys.*, vol. 31, pp. 281S-282S, May 1960.
- [6] M. R. Freeman, M. J. Brady, J. F. Smyth, *Appl. Phys. Lett.*, vol. 60, pp. 2555-2557, May 1992.
- [7] T. M. Crawford, C. T. Rogers, T. J. Silva, Y. K. Kim, "Observation of the transverse second-harmonic magneto-optic Kerr effect from Ni₈₁Fe₁₉ thin film structures," *Appl. Phys. Lett.*, vol. 68, pp. 1573-1575, March 1996.
- [8] T. J. Silva, T. M. Crawford, C. T. Rogers, Y. K. Kim, "Observation of surface oxide properties by the second harmonic magneto-optic Kerr effect in Ni₈₁Fe₁₉ films," vol. 11, 1996 OSA Technical Digest Series (Optical Society of America, Washington DC, 1996), pp. 299-301.
- [9] J. Reif, J. C. Zink, C.-M. Schneider, and J. Kirschner, "Effects of surface magnetism on optical second harmonic generation," *Phys. Rev. Lett.*, vol. 67, pp. 2878-2881, Nov. 1991.
- [10] P. H. Bryant, J. F. Smyth, S. Schultz and D. R. Fredkin, "Magnetostatic mode spectrum of rectangular ferromagnetic particles," *Phys. Rev. B*, vol. 47, pp. 11255-11262, May 1993.
- [11] C. E. Patton, Z. Frait, C. H. Wilts, "Frequency dependence of the parallel and perpendicular ferromagnetic resonance linewidth in Permalloy films, 2-36 GHz," *J. Appl. Phys.*, vol. 46, pp. 5002-5003, Nov. 1975.
- [12] M. R. Freeman, W. K. Hiebert, A. Stankiewicz, "Time-resolved scanning Kerr microscopy of ferromagnetic structures," *J. Appl. Phys.*, vol. 83, pp. 6217-6222, June 1998.
- [13] J. C. Mallinson, *The Foundations of Magnetic Recording*, 2nd ed., Academic Press: San Diego, 1993, pp. 51-52.
- [14] R.-P. Pan, H. D. Wei, Y. R. Shen, "Optical second-harmonic generation from magnetized surfaces," *Phys. Rev. B*, vol. 39, pp. 1229-1234, Jan. 1989.
- [15] D. O. Smith and K. J. Harte, "Noncoherent switching in Permalloy films," *J. Appl. Phys.*, vol. 33, pp. 1399-1413, April 1962.